PLoS one

Indocyanine Green Fluorescence Imaging for Evaluation of Uterine Blood Flow in Cynomolgus Macaque

Iori Kisu[1], Kouji Banno[1]*, Makoto Mihara[2], Li-Yu Lin[3], Kosuke Tsuji[1], Megumi Yanokura[1], Hisako Hara[2], Jun Araki[2], Takuya Iida[2], Takayuki Abe[3], Keisuke Kouyama[3], Nobuhiko Suganuma[4], Daisuke Aoki[1]

1 Department of Obstetrics and Gynecology, School of Medicine, Keio University, Tokyo, Japan, 2 Department of Plastic and Reconstructive Surgery, Graduates School of Medicine, University of Tokyo, Tokyo, Japan, 3 The Center for Clinical Research, School of Medicine, Keio University, Tokyo, Japan, 4 Department of Human Health Sciences, Kyoto University Graduate School of Medicine, Kyoto, Japan

Abstract

Background: Uterine blood flow is an important factor in uterine viability, but the number of blood vessels required to maintain viability is uncertain. In this study, indocyanine green (ICG) fluorescence imaging was used to examine uterine hemodynamics and vessels associated with uterine blood flow in cynomolgus macaque.

Methods: The uterus of a female cynomolgus macaque was cut from the vaginal canal to mimic a situation during trachelectomy or uterine transplantation surgery in which uterine perfusion is maintained only with uterine and ovarian vessels. Intraoperative uterine hemodynamics was observed using ICG fluorescence imaging under conditions in which various nutrient vessels were selected by clamping of blood vessels. A time-intensity curve was plotted using imaging analysis software to measure the T_{max} of uterine perfusion for selected blood vessel patterns. Open surgery was performed with the uterus receiving nutritional support only from uterine vessels on one side. The size of the uterus after surgery was monitored using transabdominal ultrasonography.

Results: The resulting time-intensity curves displayed the average intensity in the regions of the uterine corpus and uterine cervix, and in the entire uterus. Analyses of the uterine hemodynamics in the cynomolgus macaque showed that uterine vessels were significantly related to uterine perfusion ($P = 0.008$), whereas ovarian vessels did not have a significant relationship ($P = 0.588$). When uterine vessels were clamped, ovarian vessels prolonged the time needed to reach perfusion maximum. Postoperative transabdominal ultrasonography showed that the size of the uterus was not changed 2 months after surgery, with recovery of periodic menstruation. The cynomolgus macaque has got pregnant with favorable fetus well-being.

Conclusion: Uterine vessels may be responsible for uterine blood flow, and even one uterine vessel may be sufficient to maintain uterine viability in cynomolgus macaque. Our results show that ICG fluorescence imaging is useful for evaluation of uterine blood flow since this method allows real-time observation of uterine hemodynamics.

Introduction

The uterine artery and the ovarian/vaginal arteries, which connect with branches of the uterine artery, contribute to blood supply to the uterus, and many studies on the dominant regions of the arteries have been performed [1–4]. Radical trachelectomy is performed for young women with early cervical cancer for preservation of fertility [5] and uterine blood flow is an important factor in maintenance of uterine function in this procedure. Several studies have suggested that preservation of the uterine artery is required to maintain the potential for pregnancy and child birth [6–9]. Insufficient uterine blood flow might cause premature birth, intrauterine growth retardation, or increased susceptibility to infection [10,11], but a clear conclusion has not been reached.

Human uterine transplantation was first performed in 2000 [12]. This transplantation may permit pregnancy and child birth for women with congenital infertility, such as that produced by defects of the uterus and vagina in Mayer-Rokitansky-Küster-Hauser syndrome [13], and for those with acquired uterine infertility caused by hysterectomy due to treatment for a malignant uterine tumor [14,15], benign diseases [16] such as uterine myoma and uterine adnomyosis, and severe postpartum bleeding [17]. Uterine transplantation has also been studied in mouse [18–20], rat [21–23], pig [24,25], sheep [26,27], cynomolgus macaque [28,29], and baboon [30], but pregnancy in non-human primates after transplantation has not been achieved, including after autotransplantation. This may be due to the complicated surgical techniques, ischemic reperfusion injury, and the need for ischemic preservation. Selection

of the type and number of blood vessels required to maintain uterine blood flow may also be important. However, it is unclear how many arteries and veins are required to maintain perfusion of a transplanted uterus.

X-ray angiography and lymphoscintigraphy are used for conventional non-invasive diagnostic imaging of organs and blood/lymph vessels in vivo, but radiation exposure and the large size and cost of the equipment are problematic. To solve these problems, an indocyanine green (ICG) fluorescence imaging system was developed and used by Kitai et al. for sentinel lymph node mapping in patients with breast cancer [31]. Since lymph and blood flow can be observed in real time during surgery using ICG fluorescence imaging, the use of this approach has expanded to sentinel lymph node mapping in patients with breast cancer [32] and digestive organ cancer [34,35], evaluation of lymph channels in patients with lymphedema [35], evaluation of graft vessels [36] in coronary bypass surgery, and blood flow evaluation in reconstructed organs such as free flaps [37,38]. Thus, this angiographic technique is used widely. However, in obstetrics and gynecology, it has only been used for observation of placental communicating vessels in patients with twin-twin transfusion syndrome [39] and for observation of an angiostomy site and uterine blood flow in our experiments on uterine transplantation research [29].

In this study, we used ICG fluorescence imaging for evaluation of uterine blood flow in cynomolgus macaque to examine uterine hemodynamics, with the goal of understanding the important factors in maintenance of uterine viability in radical trachelectomy and uterine transplantation.

Methods

Animals

The study was performed in a 7-year-old female cynomolgus macaque (weight: 3.4 kg) with a regular menstrual cycle and a history of child birth. The cynomolgus macaque is anatomically and physiologically close to humans. The body and tail lengths are 38–55 and 40–65 cm, respectively, in adults, and the body weight is 5–9 kg in males and 3–6 kg in females, which are about one-tenth of those of humans. The cynomolgus macaque has a menstrual cycle of approx. 1 month and is a continuous breeder throughout the year, with a gestational period of approx. 165 days. The anatomical characteristics of the internal genital organs, including the uterus and adnexa, and vascular system of female cynomolgus macaques are similar to those of humans [28]. This study was carried out in strict accordance with the recommendations in the Guide for the Care and Use of Laboratory Animals of the National Research Council. The study protocol was approved by the Institutional Scientific Evaluation and Review Committee and the Animal Care and Use Committee of the Institute of Primate Research, Shin-Nihon-Kagaku, Kagoshima, Japan (Permit Number: SBL740-001), which is fully accredited by Association for Assessment and Accreditation of Laboratory Animal Care International (Approval No. 001404). The cynomolgus macaque was reared in each cage under the following environmental conditions: temperature of 23–29°C, humidity of 35–75%, lighting of 12 hr/day, and toys to play with all day long. The animal was also fed a commercial monkey diet once daily, with supplemental fruits and vegetables seven times weekly both pre and post operatively. Lactated Ringer's solution was administered i.v. if there was a change in the post-operative condition, such as appetite loss or dehydration.

Anesthesia

After sedation with atropine sulfate (0.02 ml/kg, i.m. injection; Mitsubishi Tanabe Pharma Corp., Tokyo, Japan) and ketamine hydrochloride (50 mg/ml aqueous solution, 0.2 ml/kg i.m.; Kamud Drugs, Tokyo, Japan), the abdomen was shaved and the animal was maintained in the supine position. The abdomen was disinfected with 70% ethanol and iodine tincture and covered with a sterilized drape. A tracheal tube was inserted and anesthesia was maintained with isoflurane inhalation (0.5–1.0%; Abbott Japan, Tokyo, Japan). During surgery, anesthesia was maintained with inhalation of a mixture of carrier gas (nitrous oxide/oxygen, 2:1) and 1% isoflurane using an inhalant anesthesia vaporizer for isoflurane (AIV-5; Kimura Medical Co., Tokyo, Japan) and equipment for general anesthesia (Kimura General Anesthesia Device Compact-15, Kimura Medical Co.) under spontaneous respiration. To compensate for fluid loss during surgery, the animal received continuous i.v. infusion of 0.163 M NaCl at 3–4 ml/kg/h. Antibiotics (dihydro-streptomycin sulfate 0.02–0.1 ml/kg i.m.; Meiji Seika, Tokyo, Japan) and buprenorphine hydrochloride (Lepetan 0.005–0.001 mg/kg i.m.; Otsuka Pharmaceutical Co., Tokyo, Japan) were administered after surgery to prevent infection and to treat pain.

Surgical Techniques

All surgical procedures were performed using sterile techniques and surgical loupes. An abdominal midline longitudinal incision (from the pubic bone up to the level of the umbilicus) was performed. The intestines were packed into the upper abdomen. After confirming that the anatomical characteristics of the internal genital organs and vascular system of the cynomolgus macaque were similar to those of humans, we cut the round ligament and examined the broad ligaments of the uterus and retroperitoneum. After identifying and exfoliating the uterine artery/vein, ovarian artery/vein, and urinary duct for visual confirmation, we then exfoliated the urinary bladder and rectum from the uterus. Assuming performance of radical trachelectomy or uterine transplantation, we treated the parametrium and paracorpium at the height of the vaginal side, rather than at the height of the uterine artery/vein because this would block blood flow from the vagina. With the uterine artery/vein and ovarian artery/vein connected to the uterus, the vaginal canal was cut. ICG (Diagnogreen 0.5%; Daiichi Pharmaceutical, Tokyo, Japan) was then intravenously administered and ICG fluorescence imaging was used to observe perfusion of the uterus in real time. After completion of observations, the base of the ovarian duct was cut so that both adnexa remained on the side of the ovarian artery/vein. Then, the uterine artery/vein on one side was cut so that only the uterine artery/vein on the other side could serve as nutrient vessels. The disconnected vaginal canal was anastomosed and suture of the retroperitoneum and repair of the round ligament were performed before closing the abdominal incision.

Intraoperative ICG Fluorescent Angiography

ICG is a dark blue-green soluble compound with a molecular weight of 774.96. ICG binds with plasma protein and is distributed to blood vessels throughout the body, taken into the liver, and excreted in bile from the liver as a free compound. ICG absorbs near infrared (IR) rays of 750–800 nm and produces strong fluorescence of 840 nm when excited [40]. However, since this wavelength is within the range of near IR, fluorescence images cannot be observed with the naked eye. The Photodynamic Eye (hereinafter referred to as PDE; Hamamatsu Photonics KK, Hamamatsu, Japan) produces excitation light of 760 nm from a light emitting diode and enables visual imaging with a CCD
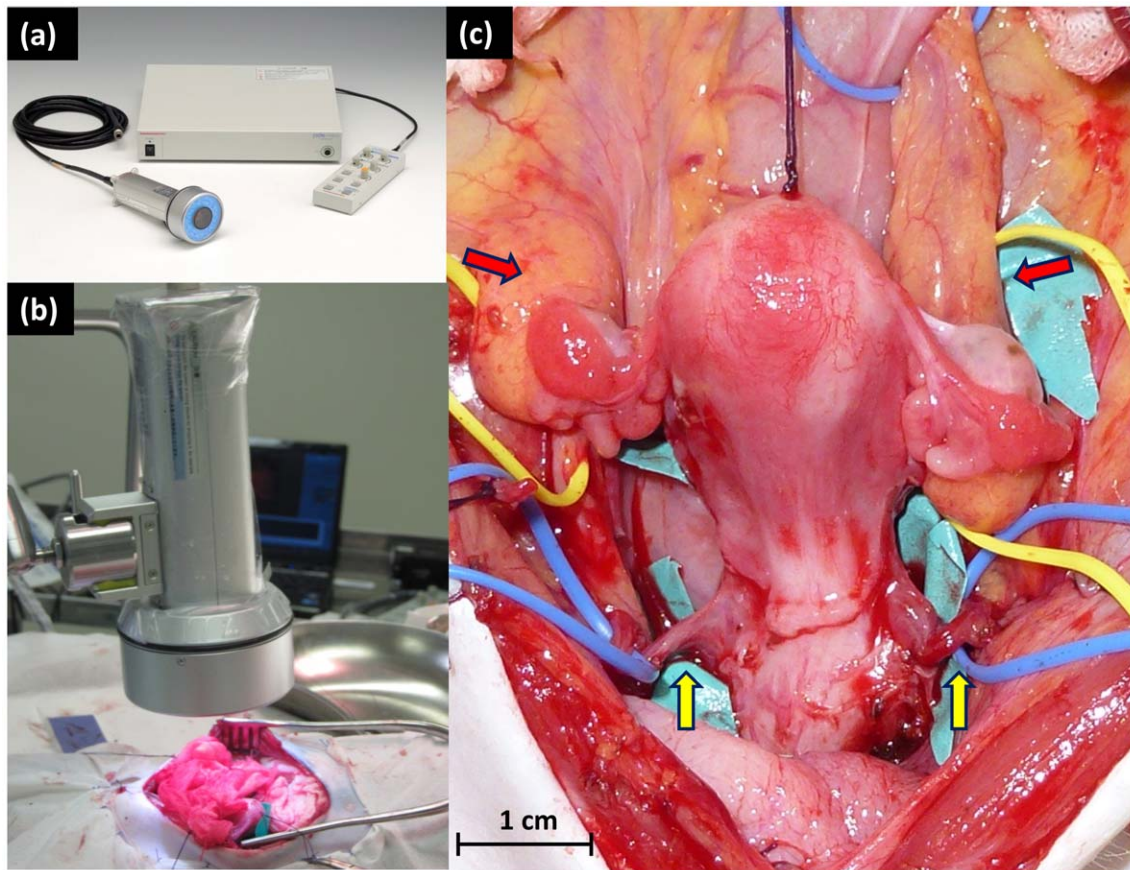
Figure 1. Preparation for intraoperative observation of uterine hemodynamics with ICG fluorescence imaging. (a) The ICG fluorescence imaging system, including the main body, camera unit, and remote controller. (b) CCD camera unit of a PDE installed at the site of surgery. (c) The uterus with a separated vaginal canal. The uterus was connected by the uterine artery/vein (yellow arrow) and ovarian artery/vein (red arrow).
doi:10.1371/journal.pone.0035124.g001

through an optical filter, which blocks excitation light of ≤820 nm and transmits only fluorescence (Fig. 1a). Using this IR observation camera system, ICG can be observed during surgery, which allows monitoring of vascular and lymph dynamics under the tissue surface and observation of the distribution of the fluorescent reagent in tissues.

Intraoperative Observation of Uterine Hemodynamics with ICG Fluorescence Imaging

ICG (0.25 mg/ml, 1 ml) was intravenously administered from the periphery. The CCD camera with a PDE was installed in the surgical field and real-time images of uterine perfusion during surgery were obtained by ICG fluorescence imaging and observed on the monitor of a laptop computer (Fig. 1b). Uterine hemodynamics was observed after clamping blood vessels to examine perfusion from selected vessels, as shown in Table 1. Uterine perfusion was examined for vessel patterns with 6 vessels (A), 4 vessels (B), 2 vessels, including uterine vessels only (C), ovarian vessels only (D), a pair of uterine and ovarian vessels on the same side (E) and the opposite side (F), one ovarian vessel (G), and one uterine vessel (H) (Table 1). Other than for pattern A, hemodynamics was observed under conditions in which the vaginal canal was completely separated from the uterus (Fig. 1c). All experiments were performed with systolic blood pressure 90–99 mmHg and diastolic blood pressure 40–49 mmHg to ensure

that the ICG fluorescence distribution was not affected by blood pressure.

ROI Software

Images were imported into a computer and changes in fluorescence intensity were measured over time using image intensity analysis software (ROI [Region Of Interest] software: Hamamatsu Photonics KK). This software analyzes the intensity of images on a scale of 0 to 256. Changes in average intensity over time in a given region are shown numerically and can be plotted graphically using the software (Fig. 2a, Fig. S1). In ICG images for the patterns of blood vessels shown in Table 1, individual regions were defined using the ROI software to include the uterine corpus and cervix. These data and the average intensity in the entire uterine region, including both corpus and cervix regions, were plotted as time-intensity curves (Fig. 2b). The time (s) at which the intensity reached a maximum (T_{max}) was measured as a marker of the blood supply to the uterus. The half-life of the highest intensity ($T_{1/2}$) was also measured for evaluation of uterine blood perfusion.

Postoperative Observation

Postoperative transabdominal ultrasonography and trans-vaginal observation with an endoscope were performed to monitor the uterus perfused only by uterine vessels on one

Table 1. Patterns of selected blood vessels used for uterine perfusion observed by ICG fluorescence imaging.

Pattern	Uterine vessels		Ovarian vessels		Vaginal vessels		Number of patent vessels	
	Rt.	Lt.	Rt.	Lt.	Rt.	Lt.	Uterine	Ovarian
A	+	+	+	+	+	+	2	2
B	+	+	+	+			2	2
C	+	+					2	0
D			+	+			0	2
E	+		+				1	1
F	+			+			1	1
G			+				0	1
H	+						1	0

+: Vessel patency.
doi:10.1371/journal.pone.0035124.t001

side. Postoperative resumption of menstruation was also monitored.

Statistical Analysis

A linear regression model was constructed for examining correlations between the outcome measurement of uterine perfusion time and uterine and ovarian vessels as two explanatory variables. The significance level was 5% and all tests were two-sided. The analyses of this study were performed with SAS statistical software, version 9.2.

Results

Intraoperative ICG Fluorescent Angiography

ICG fluorescence imaging with a PDE enabled intraoperative real-time observation of uterine hemodynamics. Analysis of the temporal changes in the normal uterus (Fig. 3) showed that ICG expanded from the uterine cervix to the uterine corpus through the uterine artery and was excreted from the uterus through the ovarian vein when full blood flow was observed in the entire uterus.

Changes in Perfusion Intensity Over Time

Temporal changes in perfusion intensity obtained by ICG fluorescence imaging were recorded with ROI software for all patterns of blood vessels. The resulting time-intensity curves (Fig. 4) showed the average intensity in the regions of the uterine corpus and uterine cervix, and in the entire uterus. The time needed to reach perfusion maximum, marked as T_{max}, and the time of perfusion decay by half, $T_{1/2}$, were obtained from the curve (Table 2). When all three supplying vessels–uterine vessels, ovarian vessels, and vaginal vessels– were patent, the baseline averaged T_{max} was 14.8 seconds and $T_{1/2}$ was 53.4 seconds. The results from subsequent patterns were also obtained according to different vessels and their numbers of patency. Under the same pattern of selected supplying vessels, the curves for the corpus and cervix illustrated similar tendencies of perfusion.

It was noted, from Table 2, that T_{max} was shorter for patterns with increased numbers of uterine vessels patency. Furthermore, in patterns D and G, which only included ovarian vessels, values of T_{max} and $T_{1/2}$ were strikingly higher when compared with other patterns, suggesting poor uterine perfusion. T_{max} did not differ remarkably between pattern E, in which a uterine artery/vein and ovarian artery/vein on the same side were selected, and pattern F, in which those on opposite sides
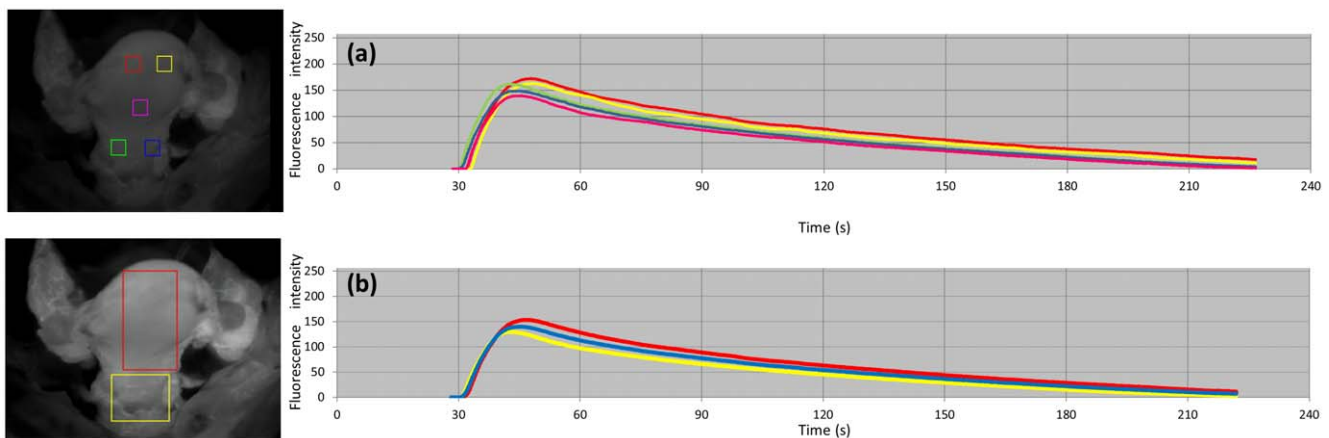

Figure 2. Time-intensity curves prepared by ROI software to show temporal changes in ICG fluorescence intensity (Pattern A). (a) Temporal changes in intensity in 5 specified regions (red: right uterine corpus, yellow: left uterine corpus, green: right uterine cervix, blue: left uterine cervix, pink: uterine isthmus) (b) Temporal changes in average intensity in the uterine corpus (red), uterine cervix (yellow) regions, and the whole uterine region including the corpus and cervix regions (blue).
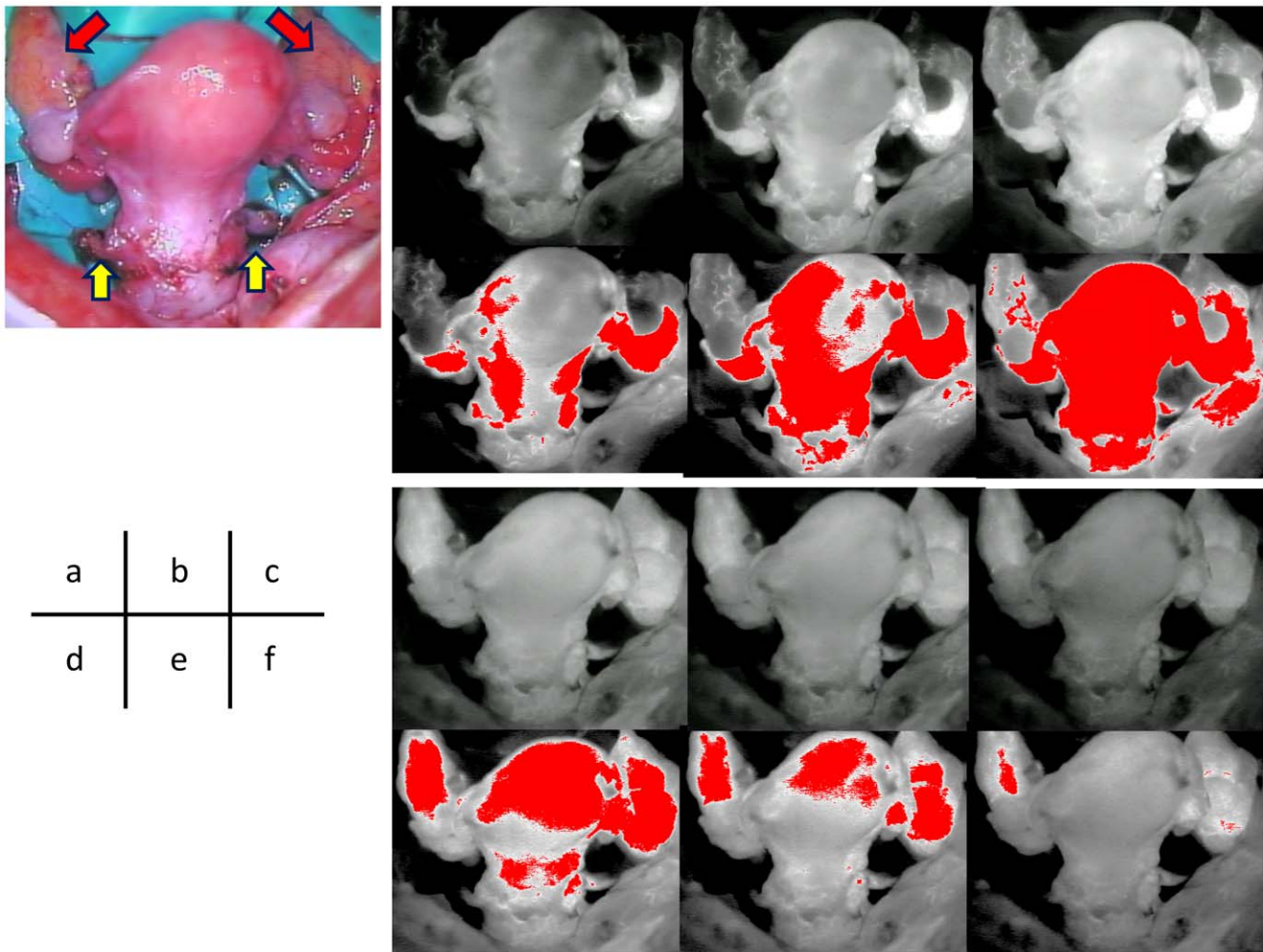doi:10.1371/journal.pone.0035124.g002

Figure 3. Temporal distribution of uterine blood flow observed by ICG fluorescence imaging after (a) 5 s, (b) 8 s, (c) 12 s, (d) 35 s, (e) 45 s, and (f) 60 s. Upper: ICG fluorescence imaging; lower: Regions with fluorescence intensity ≥100 are shown in red. Uterine artery/vein (yellow arrow) and ovarian artery/vein (red arrow).
doi:10.1371/journal.pone.0035124.g003

were selected. Multiple regression analysis of association between uterine perfusion and two nutrient vessels in the cynomolgus macaque showed that uterine vessels were significantly related to T_{max} (P = 0.008), but that ovarian vessels were not significantly related to T_{max} (P = 0.588).

Postoperative Evaluation of the Uterus

Findings on transabdominal ultrasonography showed that the size of the uterine corpus was 25.2×13.1 mm (long axis × anteroposterior diameter) at the time of surgery, and this size showed no major change 2 months after surgery (25.0×13.8 mm) (Fig. 5a,b). The RI, PI, and PSV of the right uterine artery using Doppler ultrasonography were 0.615, 0.928, and 28.2 cm/s, respectively, preoperatively; and 0.618, 0.989, and 32.5 cm/s, respectively, at 2 months after surgery, again showing no major change. Transvaginal observation with an endoscopy performed showed a reddish uterine cervix. Periodic menstruation resumed on postoperative day 44.

The cynomolgus macaque underwent natural mating after three normal menstrual cycles. At 37 days after mating, transabdominal ultrasonography revealed a viable fetus with crown-rump length 12.3mm and regular fetal heart beat (Fig. 5c). The right uterine

artery flow using Doppler ultrasonography was satisfactory and no collateral vessels toward the uterus were shown (Fig. 5d). At 68 days after mating, the pregnancy is ongoing with favorable fetus well-being.

Discussion

ICG fluorescence imaging is an angiographic technique that is simple to use and is minimally invasive. As a visualization agent, ICG has the advantages of no uptake by peripheral tissues, rapid elimination from blood, potential for repeated use in tests, and comparatively high safety with few side effects. However, ICG cannot be used in patients with iodine allergy. We showed the value of ICG fluorescence imaging for confirming a site of anastomosis and blood flow in a transplanted uterus of cynomolgus macaque [29]. However, the hemodynamics and nutrient vessels of the uterus have not been previously examined using ICG fluorescence imaging. Therefore, with the aim of examining the hemodynamics in the uterus, we investigated differences in uterine perfusion using different blood vessels that supply nutrients to the uterus using ICG fluorescence imaging during surgery in a cynomolgus macaque.
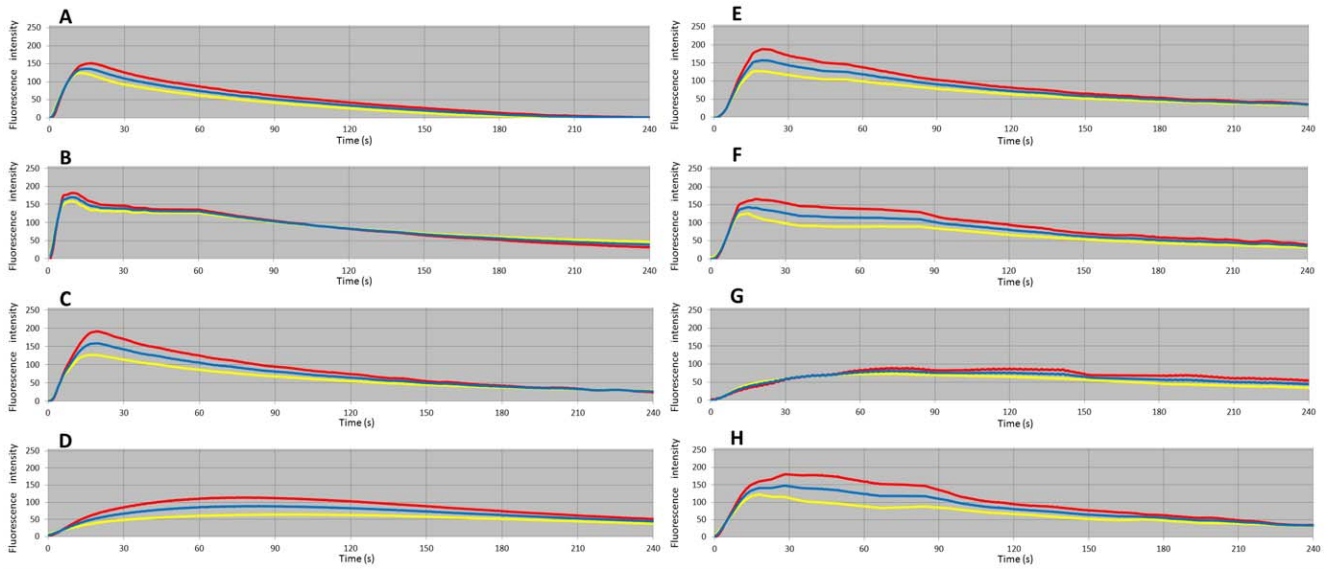
Figure 4. Time-intensity curves for different patterns of vessels for uterine perfusion. A Bilateral uterine + ovarian + vaginal vessels. B Bilateral uterine + ovarian vessels. C Bilateral uterine vessels. D Bilateral ovarian vessels. E Right uterine vessel + right ovarian vessel. F Right uterine vessel + left ovarian vessel. G Right ovarian vessel, H right uterine vessel. Red: uterine corpus, yellow: uterine cervix, blue: average of uterine corpus and cervix.
doi:10.1371/journal.pone.0035124.g004

The uterus has six supply vessels (ovarian, uterine, and vaginal). In abdominal radical trachelectomy, only 2 ovarian vessels have been used to maintain blood supply to the uterus in some cases in which pregnancy and child birth were subsequently successful. Thus, these reports suggest that the ovarian vessels, or 2 out of the 6 uterine vessels, are required to maintain uterine viability [6]. In contrast, it has also been suggested that premature birth or intrauterine growth retardation might occur if the uterine arteries are not preserved, and recent reports support the preservation of uterine artery [7]. For organ perfusion, the artery system that provides the blood supply and the vein system that is responsible for perfusion are both important. The uterine arteries are the main contributors to the blood supply to the uterus. However, in uterine blood perfusion, it is difficult to determine which veins (ovarian vessels, uterine vessels, and deep uterine vein) [41,42] are most important. In uterine transplantation experiments, Enskog et al. used the ovarian vein and Kisu et al. used the deep uterine vein

Table 2. T_{max} and $T_{1/2}$ values in time-intensity curves for perfusion of the entire uterine region with different patterns of blood vessels.

Pattern	T_{max} (s)	$T_{1/2}$ (s)
A	14.8	53.4
B	11.6	104.6
C	19.7	73.4
D	75	166.8
E	19.8	89.4
F	18.1	118.6
G	72.6	186.4
H	28	105.8

doi:10.1371/journal.pone.0035124.t002

for uterine perfusion. The temporal distribution of uterine blood flow observed by ICG fluorescence imaging in the current study showed uterine hemodynamics in which the blood flow from the uterine artery perfused mainly to ovarian veins, rather than uterine veins. This suggests that ovarian veins mainly contribute to uterine perfusion during surgery because the diameters of uterine veins are small and some patients may have no uterine veins. Postoperatively, uterine perfusion was achieved only with one uterine vein, and menstruation resumed. Thus, it appears that only one uterine vein is sufficient to maintain the viability of the uterus in some cases. However, further data are required to determine whether one uterine vein is enough to maintain uterus viability in all cases.

T_{max} for intensity was used as a marker of the blood supply to the uterus. The $T_{1/2}$ of intensity could also have been used as a marker of uterine perfusion, but this marker may be inappropriate because it could be affected by a decrease in the plasma elimination rate due to uterine blood supply and repeated administration of ICG, in addition to uterine perfusion. The results based on T_{max} suggested that the uterine blood supply was mainly controlled by uterine vessels, and not by ovarian vessels, and was favorable with a higher number of connected vessels. Menstruation in this cynomolgus macaque was recovered after surgery, showing uterine viability. This suggests that one uterine vessel may be sufficient to maintain uterine perfusion in cynomolgus macaque. However, it may be better to keep two uterine vessels because it may become difficult to maintain the viability of the uterus if a single uterine vessel is stenosed or obstructed. In addition, T_{max} was clearly longer when the blood supply was provided by ovarian vessels only. Therefore, uterine blood supply in trachelectomy and uterine transplantation may require perfusion with at least two uterine arteries.

ICG fluorescence imaging enabled real-time observation of uterine hemodynamics. This method should be useful for confirmation of blood flow in preserved uterine arteries or anastomosed vessels and for evaluation of uterine perfusion in trachelectomy and uterine transplantation. However, this study
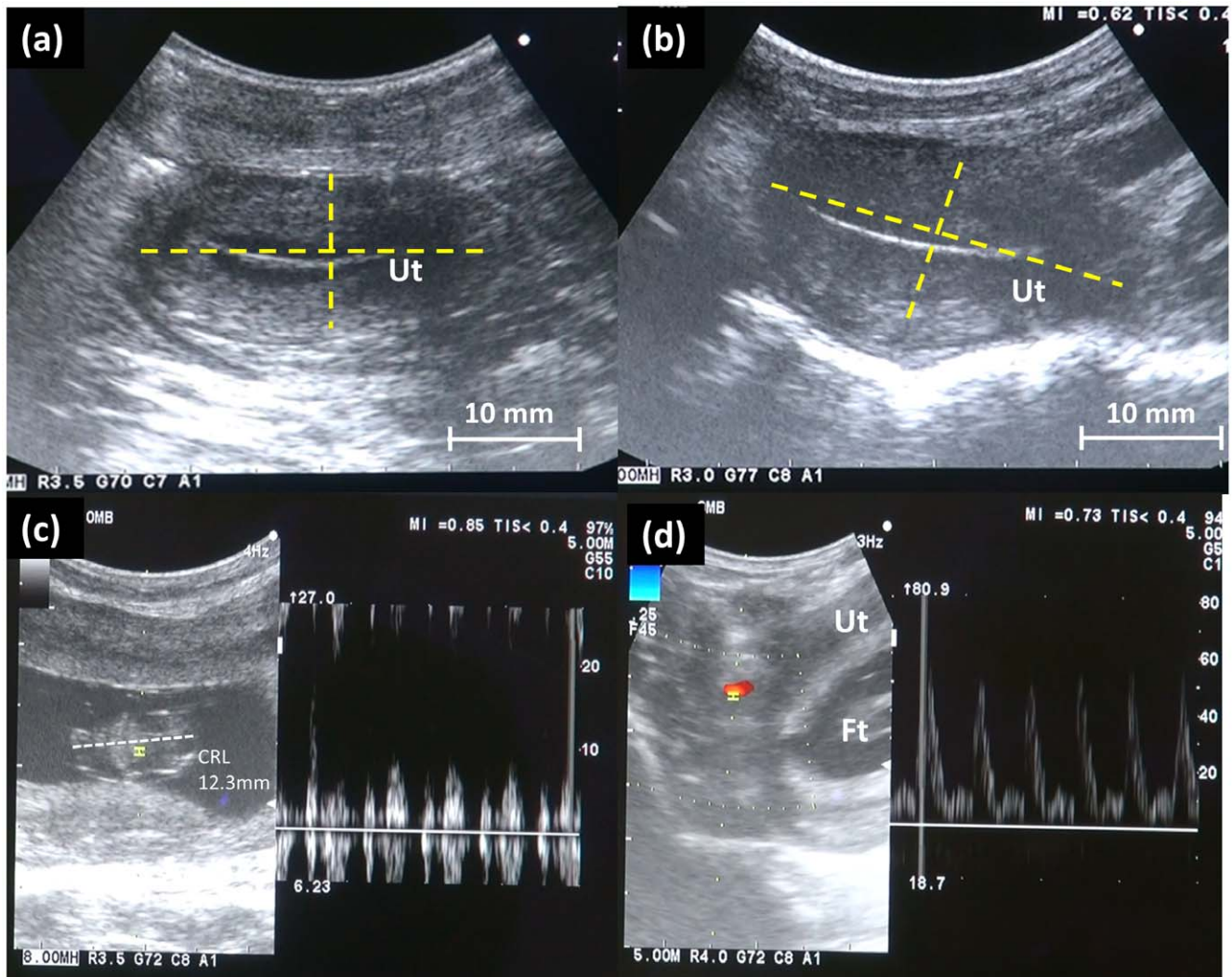
Figure 5. Postoperative evaluation of the uterus. (a) Transabdominal ultrasonography at the time of surgery showed the size of the uterine corpus was 25.2 × 13.1 mm (long axis × anteroposterior diameter) (b) The size of uterine corpus at 2 months after surgery was 25.0 × 13.8 mm, showing no major change in the size of the uterus. Ut: uterus. (c) At 37 days after mating, transabdominal ultrasonography revealed a viable fetus with crown-rump length 12.3mm and regular fetal heart beat. (d) The right uterine artery flow using Doppler ultrasonography was satisfactory and no collateral vessels toward the uterus were shown. Ut: uterus, Ft: fetus.
doi:10.1371/journal.pone.0035124.g005

was performed in the uterus of a cynomolgus macaque and the results may differ from those in a human uterus, although cynomolgus macaque is a similar primate to humans. In addition, only one primate animal was examined in this study due to ethical considerations regarding animal protection, and this makes it difficult to assess the reproducibility of our results. Therefore, we exhaustively searched the literature for studies on irregularity of uterine blood flow, and found that uterine blood flow can be affected by menstrual cycle [2], estrogen/progesterone ratio [43], ovarian artery-to-uterine artery anastomoses in women undergoing fibroid embolization [4], uterine area [2,3,44], supplementary flow to the uterus from the vaginal artery [3,44], and a preserved or non-preserved uterine artery in trachelectomy [6,7,10,45]. However, no data are available on the reproducibility in one subject or for the irregularity of uterine blood flow measured among individuals under the same conditions. Therefore, the results in the current study should be interpreted carefully with regard to reproducibility. Changes in

uterine hemodynamics in pregnant subjects also require examination.

The current study was performed as an exploratory investigation of ICG fluorescence imaging for evaluation of uterine blood flow and further data collection is required. However, we conclude that intraoperative real-time observation using ICG fluorescence is useful for evaluation of uterine hemodynamics. Most importantly, our results suggested that uterine vessels, rather than ovarian vessels, are responsible for uterine flood flow, and that even one uterine vessel may be sufficient to maintain uterine viability.

Supporting Information

Figure S1   Supplementary video image for time-intensity curves prepared by ROI software to show temporal changes in ICG fluorescence intensity.
(WMV)

Acknowledgments

Author Contributions

Conceived and designed the experiments: IK. Performed the experiments: KB MM KT MY HH JA TI NS DA. Analyzed the data: LL TA KK. Contributed reagents/materials/analysis tools: IK KB MM LL KT MY HH JA TI TA KK NS DA. Wrote the paper: IK.

References

1. Einer-Jensen N, Cicinelli E, Galantino P, Pinto V, Barba B (2001) Preferential vascular-based transfer from vagina to the corpus but not to the tubal part of the uterus in postmenopausal women. Hum Reprod 16: 1329–1333.
2. Cicinelli E, Einer-Jensen N, Barba B, Luisi D, Alfonso R, et al. (2004) Blood to the cornual area of the uterus is mainly supplied from the ovarian artery in the follicular phase and from the uterine artery in the luteal phase. Hum Reprod 19: 1003–1008.
3. Palacios Jaraquemada JM, García Mónaco R, Barbosa NE, Ferle L, Iriarte H, et al. (2007) Lower uterine blood supply: extrauterine anastomotic system and its application in surgical devascularization techniques. Acta Obstet Gynecol Scand 86: 228–234.
4. Razavi MK, Wolanske KA, Hwang GL, Sze DY, Kee ST, et al. (2002) Angiographic classification of ovarian artery-to-uterine artery anastomoses: initial observations in uterine fibroid embolization. Radiology 224: 707–712.
5. Dursun P, LeBlanc E, Nogueira MC (2007) Radical vaginal trachelectomy (Dargent's operation): a critical review of the literature. Eur J Surg Oncol 33: 933–941.
6. Sieunarine K, Moxey P, Boyle DC, Ungar L, Lindsay I, et al. (2005) Selective vessel ligation in the pelvis: an invaluable tool in certain surgical procedures. Int J Gynecol Cancer 15: 967–973.
7. Al-Niaimi AN, Einstein MH, Perry L, Hartenbach EM, Kushner DM (2011) Uterine artery sparing robotic radical trachelectomy (AS-RRT) for early cancer of the cervix. Int J Gynaecol Obstet 112: 76–80.
8. Cibula D, Slama J, Fischerova D (2008) Update on abdominal radical trachelectomy. Gynecol Oncol 111: S111–115.
9. Abu-Rustum NR, Sonoda Y (2007) Fertility-sparing radical abdominal trachelectomy for cervical carcinoma. Gynecol Oncol 104: 56–59.
10. Klemm P, Tozzi R, Köhler C, Hertel H, Schneider A (2005) Does radical trachelectomy influence uterine blood supply? Gynecol Oncol 96: 283–286.
11. Ungár L, Smith JR, Pálfalvi L, Del Priore G (2006) Abdominal radical trachelectomy during pregnancy to preserve pregnancy and fertility. Obstet Gynecol 108: 811–814.
12. Fageeh W, Raffa H, Jabbad H, Marzouki A (2002) Transplantation of the human uterus. Int J Gynaecol Obstet 76: 245–251.
13. Saravelous SH, Cocksedge KA, Li TC (2008) Prevalence and diagnosis of congenital uterine anomalies in women with rproductive failure: a critical appraisal. Hum Reprod Update 14: 415–429.
14. Quinn MA, Benedet JL, Odicino F, Maisonneuve P, Beller U, et al. (2006) Carcinoma of the uterine cervix. FIGO 26th annual report on the results on treatment in gynaecological cancer. Int Gynecol Obstet 95: S43–S103.
15. Creasman WT, Odicino F, Maisonneuve P, Quinn MA, Beller U, et al. (2006) Carcinoma of the corpus uteri. FIGO 26th annual report on the results on treatment in gynaecological cancer. Int Gynecol Obstet 83: S105–S143.
16. Marshall LM, Spiegelman D, Barbieri RL, Goldman MB, Manson JE, et al. (1997) Variation in the incidence of uterine leiomyoma among premenopausal women by age and race. Obstet Gynecol 90: 967–973.
17. Díaz-García C, Johannesson L, Enskog A, Tzakis A, Olausson M, et al. (2012) Uterine transplantation research: laboratory protocols for clinical application. Mol Hum Reprod 18: 68–78.
18. Racho El-Akouri R, Kurlberg G, Brannstrom M (2003) Successful uterine transplantation in the mouse: pregnancy and post-natal development of offspring. Hum Reprod 18: 2018–2023.
19. Racho El-Akouri R, Wranning CA, Molne J, Kurlberg G, et al. (2003) Pregnancy in transplanted mouse uterus after long-term cold ischaemic preservation. Hum Reprod 18: 2024–2030.
20. El-Akouri RR, Molne J, Groth K, Kurlberg G, Brännström M (2006) Rejection patterns in allogeneic uterus transplantation in the mouse. Hum Reprod 21: 436–442.
21. Wranning CA, Akhi SN, Kurlberg G, Brännström M (2008) Uterus transplantation in the rat: model development, surgical learning and morphological evaluation of healing. Acta Obstet Gynecol Scand 87: 1239–1247.
22. Wranning CA, Akhi SN, Diaz-Garcia C, Brännström M (2011) Pregnancy after syngeneic uterus transplantation and spontaneous mating in the rat. Human Reprod 26: 553–558.
23. Diaz-Garcia C, Akhi SN, Wallin A, Pellicer A, Brännström M (2010) First report on fertility after allogeneic uterus transplantation. Acta Obstet Gynecol Scand 89: 1491–1494.
24. Avison DL, DeFaria W, Tryphonopoulos P, Tekin A, Attia GR, et al. (2009) Heterotopic uterus transplantation in a swine model. Transplantation 88: 465–469.
25. Wranning CA, El-Akouri RR, Lundmark C, Dahm-Kahler P, Molne J, et al. (2006) Auto-transplantation of the uterus in the domestic pig (Sus scrofa): Surgical technique and early reperfusion events. J Obstet Gynaecol Res 32: 358–67.
26. Ramirez ER, Ramirez Nessetti DK, Nessetti MB, Khatamee M, Wolfson MR, et al. (2011) Pregnancy and outcome of uterine allotransplantation and assisted reproduction in sheep. J Minim Invasive Gynecol 18: 238–245.
27. Wranning CA, Marcickiewicz J, Enskog A, Dahm-Kähler P, Hanafy A, et al. (2010) Fertility after autologous ovine uterine-tubal-ovarian transplantation by vascular anastomosis to the external iliac vessels. Hum Reprod 25: 1973–1979.
28. Kisu I, Mihara M, Banno K, Hara H, Yamamoto T, et al. (2012) A new surgical technique of uterine auto-transplantation in cynomolgus monkey: preliminary report about two cases. Arch Gynecol Obstet 285: 135–140.
29. Mihara M, Kisu I, Hara H, Iida T, Yamamoto T, et al. (2011) Uterus autotransplantation in cynomolgus macaques: intraoperative evaluation of uterine blood flow using indocyanine green. Hum Reprod 26: 3019–3027.
30. Enskog A, Johannesson L, Chai DC, Dahm-Kahler P, Marcickiewicz J, et al. (2010) Uterus transplantation in the baboon: methodology and long-term function after auto-transplantation. Hum Reprod 25: 1980–1987.
31. Kitai T, Inomoto T, Miwa M, Shikayama T (2005) Fluorescence navigation with indocyanine green for detecting sentinel lymph nodes in breast cancer. Breast Cancer 12: 211–215.
32. Hojo T, Nagao T, Kikuyama M, Akashi S, Kinoshita T (2010) Evaluation of sentinel node biopsy by combined fluorescent and dye method and lymph flow for breast cancer. Breast 19: 210–213.
33. Miyashiro I, Miyoshi N, Hiratsuka M, Kishi K, Yamada T, et al. (2008) Detection of sentinel node in gastric cancer surgery by indocyanine green fluorescence imaging: comparison with infrared imaging. Ann Surg Oncol 15: 1640–1643.
34. Noura S, Ohue M, Seki Y, Tanaka K, Motoori M, et al. (2010) Feasibility of a lateral region sentinel node biopsy of lower rectal cancer guided by indocyanine green using a near-infrared camera system. Ann Surg Oncol 17: 144–151.
35. Yamamoto T, Yamamoto N, Doi K, Oshima A, Yoshimatsu H, et al. (2011) Indocyanine green-enhanced lymphography for upper extremity lymphedema: a novel severity staging system using dermal backflow patterns. Plast Reconstr Surg 128: 941–947.
36. Handa T, Katare RG, Sasaguri S, Sato T (2009) Preliminary experience for the evaluation of the intraoperative graft patency with real color charge-coupled device camera system: an advanced device for simultaneous capturing of color and near-infrared images during coronary artery bypass graft. Interact Cardiovasc Thorac Surg 9: 150–154.
37. Azuma R, Morimoto Y, Masumoto K, Nambu M, Takikawa M, et al. (2008) Detection of skin perforators by indocyanine green fluorescence nearly infrared angiography. Plast Reconstr Surg 122: 1062–1067.
38. Prantl L, Schmitt S, Geis S, Tsui TY, Lamby P, et al. (2008) Contrast harmonic ultrasound and indocyanine-green fluorescence video angiography for evaluation of dermal and subdermal microcirculation in free parascapular flaps. Clin Hemorheol Microcirc 38: 105–118.
39. Ishiyama A, Kim K, Yamashita H, Miyamoto Y, Enosawa S, et al. (2011) New fluorescence endoscope for use in twin-twin transfusion syndrome: in vivo visualization of placental blood vessels. Med Eng Phys 33: 381–385.
40. Bensori RC, Kunes HA (1978) Fluorescence properties of indocyanine green as related to angiography. Phys Med Biol 23: 159–163.
41. Yabuki Y, Asamoto A, Hoshiba T, Nishimoto H, Nishikawa Y, et al. (2000) Radical hysterectomy: An anatomic evaluation of parametrial dissection. Gynecol Oncol 77: 155–163.
42. Yabuki Y, Sasaki H, Hatakeyama N, Murakami G (2005) Discrepancies between classic anatomy and modern gynecologic surgery on pelvic connective tissue structure: harmonization of those concepts by collaborative cadaver dissection. Am J Obstet Gynecol 193: 7–15.
43. DeZiegler D, Bessis R, Frydman R (1991) Vascular resistance of uterine arteries: physiological effects of estradiol and progesterone. Fertil Steril 55: 775–779.
44. Cicinelli E, Einer-Jensen N, Galantino P, Alfonso R, Nicoletti R (2004) The vascular cast of the human uterus: from anatomy to physiology. Ann N Y Acad Sci 1043: 19–26.
45. Abu-Rustum NR, Sonoda Y, Black D, Levine DA, Chi DS, et al. (2006) Fertility-sparing radical abdominal trachelectomy for cervical carcinoma: technique and review of the literature. Gynecol Oncol 103: 807–813.